Available online at www.sciencedirect.com
ScienceDirect
ELSEVIER
International Journal of Solids and Structures 44 (2007) 2715–2731
INTERNATIONAL JOURNAL OF SOLIDS and STRUCTURES
www.elsevier.com/locate/ijsolstr

Interplay of size effects in concrete specimens under tension studied via computational stochastic fracture mechanics

M. Vořechovský *

Institute of Structural Mechanics, Brno University of Technology, Faculty of Civil Engineering, Veveří 95, 602 00 Brno, Czech Republic

Received 21 April 2006; received in revised form 4 August 2006
Available online 22 August 2006

Abstract

We attempt the identification, study and modeling of possible sources of size effects in concrete structures acting both separately and together. We are particularly motivated by the interplay of several identified scaling lengths stemming from the material, boundary conditions and geometry. Methods of stochastic nonlinear fracture mechanics are used to model the well published results of direct tensile tests of dog-bone specimens with rotating boundary conditions. Firstly, the specimens are modeled using microplane material law to show that a large portion of the dependence of nominal strength on structural size can be explained deterministically. However, it is clear that more sources of size effect play a part, and we consider two of them. Namely, we model local material strength using an autocorrelated random field attempting to capture a statistical part of the complex size effect, scatter inclusive. In addition, the strength drop noticeable with small specimens which was obtained in the experiments is explained by the presence of a weak surface layer of constant thickness (caused e.g., by drying, surface damage, aggregate size limitation at the boundary, or other irregularities). All three named sources (deterministic-energetic, statistical size effects, and the weak layer effect) are believed to be the sources most contributing to the observed strength size effect; the model combining all of them is capable of reproducing the measured data. The computational approach represents a marriage of advanced computational nonlinear fracture mechanics with simulation techniques for random fields representing spatially varying material properties. Using a numerical example, we document how different sources of size effects detrimental to strength can interact and result in relatively complex quasibrittle failure processes. The presented study documents the well known fact that the experimental determination of material parameters (needed for the rational and safe design of structures) is very difficult for quasibrittle materials such as concrete.

Keywords: Size effect; Scaling; Random field; Weak boundary; Crack band; Microplane model; Dog-bone specimens; Quasibrittle failure; Crack initiation; Stochastic simulation; Characteristic length

1. Introduction

This paper studies the complex size effect on the nominal strength of concrete structures. The target is to identify possible sources of size effect, study them and model them together in one complex model. We want to

* Tel.: +420 5 4114 7370; fax: +420 5 4124 0994.
E-mail address: vorechovsky.m@fce.vutbr.cz

0020-7683/$ - see front matter
doi:10.1016/j.ijsolstr.2006.08.019

show how the different sources interact with each other. We are particularly interested in the interaction of different material length scales and the effect of such interaction on size effect.

Topically, the most related work by other authors is the paper by Gutiérrez and de Borst (2002), dealing with deterministic and statistical lengths and their role in size effect. Several very influential works were produced in the 1990s (Carmeliet and Hens, 1994; Carmeliet and de Borst, 1995). They combined a simple nonlocal damage model and simulation of a bi-variate random field of material properties (damage threshold and strain softening) within a single finite element computational model, and studied the two different length parameters: the characteristic length of the nonlocal damage model, and the correlation distance for the random field. The illustrated example presenting finite-element analyses of direct-tension tests has shown that the specimen exhibits structural behavior that is representative of nonsymmetrical deformation, with a nonlinear stress–displacement curve. It has also shown that the two sources of size effect can be modeled satisfactorily well. Their model utilizes experience gained from a paper by Mazars et al. (1991), who also studied the two sources of size effect in cementitious materials using a continuous damage model, and compared the results with experiments on both notched and unnotched bending beams. Unfortunately, they did not consider more than one random property, and ignored its spatial correlation. The interplay of deterministic and statistical size effects is one of the central topics in Vořechovský (2004b). Some analytical results supported by a large computational case study of the Malpasset dam failure are published in Vořechovský et al. (2005) and Bažant et al. (in press).

In a very recent paper, Gutiérrez (2006) presented a method for direct evaluation of the size sensitivity of the reliability index β. The quasibrittle solid is modeled by a gradient-enhanced model with strength described by a random field. The sensitivity analysis is performed on a numerical example involving a notched specimen under uniaxial tension over the size range of 1:2 and with three different correlation lengths of the random strength field. An expected trend of decreasing reliability is observed for increasing structural size. The method is based on the design point search in standardized Gaussian space U of random variables, which are used to represent random material properties (related by Nataf's probabilistic transformation (Liu and Der Kiureghian, 1986)). The design point is the closest point from origin in the U-space (with a distance β) corresponding to the most probable mode of failure. Therefore, the method provides good results in cases when only one failure mode dominates such as in the case of e.g., a three point bending test of notched specimens. In case of a small (relatively ductile) structure without notches, multiple failure modes can be expected, and knowledge of correlation between them would be required to assess sensitivity. Moreover, Nataf's transformation (based only on marginal distributions and covariances) does not provide a unique relationship between the original (nonGaussian) space of correlated variables and the standardized Gaussian space U in which the sensitivity is computed. The aforementioned difficulties may support the choice of the classical Monte Carlo simulation approach for studying the complex size effect on structural strength (statistical part inclusive), as it is presented here.

Even though we have the ambition to study the size effect phenomena in general terms, we have decided to illustrate the problem using a particular example for the sake of easier comprehension and transparency. In particular, we study the well published experimental results of direct tensile tests on dog-bone specimens with rotating boundary conditions of varying size (size range 1:32) performed by van Vliet and van Mier and summarized in the PhD thesis by van Vliet (2000) and in papers by van Vliet and van Mier (1998, 1999, 2000a,b), van Mier and van Vliet (2003) and Dyskin et al. (2001). We are interested in the series of "dry" concrete specimens A to F (dimension D varying from 50 to 1600 mm, see Fig. 1); a series accompanied by tensile splitting verification tests. The paper attempts an explanation of the complex size effect on the mean and variance of nominal strength by a combination of random field simulation of local material properties and "weak boundary" effects, and a nonlinear fracture mechanics simulation based on a cohesive crack model. There has been much effort expended on different explanations of the experimentally obtained size effects on strength from several different points of view. Firstly, the effect of a nonuniform distribution of strains in the smallest cross-section was studied using simple linear constitutive law (van Vliet and van Mier, 1999, 2000a), and a separation of structural and material size effects was discussed. van Vliet and van Mier (1999) argue that most of the experimentally observed size effect could be explained by strain/stress gradients that develop due to several reasons. The results were also compared to the Weibull theory (Weibull, 1939) based on the weakest-link model which was found to fit the mean nominal strength of sizes B to F (van Vliet and van Mier, 1998, 1999,

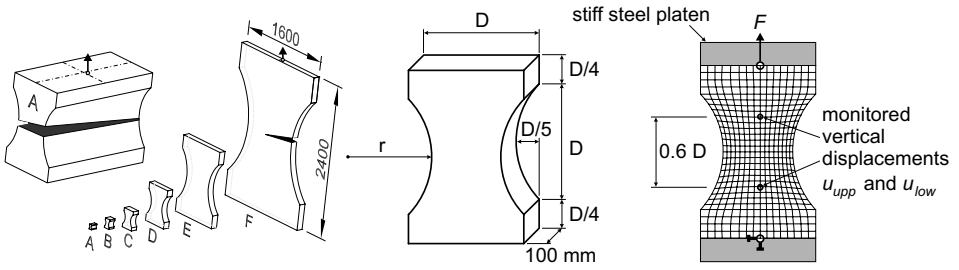

Fig. 1. Dog-bone specimens tested by van Vliet and van Mier (1998): series A to F, 2D modeled in ATENA software.

2000a,b; van Mier and van Vliet, 2003). Unfortunately, the slope of the mean size effect curve corresponds to a Weibull modulus of 6, which does not coincide with the measured scatter of strengths at each size. However, this is required in the Weibull type of size effect. Secondly, the effect of Gaussian stress fluctuation with non-uniform loading was studied by Dyskin et al. (2001), and the developed model, employing a limiting distribution of independent Gaussian variables with linear trend, agrees with the experimental data very well. Van Mier and van Vliet also compared the data to the "Delft lattice model" using a simple local elastic-brittle material with both regular and random lattices, and they obtained good results. The statistical part of experimentally obtained size effect has recently been modeled by Lehký and Novák (2002), employing a limiting distribution of independent Weibull variables describing the distribution of strength.

In this paper, the author firstly tries to explain the mean size effect curve with deterministic effects (not taking into account the local material strength with a random field). There is a partial explanation of the decreasing slope of the mean size effect curve (MSEC) in a double-logarithmic plot (nominal strength versus characteristic size). However, the strong decrease in the mean strength of the smallest specimen A is believed to be sufficiently captured by a modeled weak surface layer with a thickness of about 2 mm. A parametric study of the influence of "weak layer" thickness and the percentage reduction in the layer's strength compared to the bulk strength will be presented with regard to the resulting MSEC. Next, the author approximates the local material strength via an autocorrelated random field, attempting to capture the statistical size effect, scatter inclusive, and finally combine all sources together.

2. Experiments

The experiments by van Vliet and van Mier are well documented in the seven references cited in the introduction. We will briefly mention only those necessary data needed to explain the computational model: all other details can be found in the cited publications. Dog-bone shaped specimens were loaded in uniaxial tension with geometrically scaled eccentricity from the vertical axis of symmetry $e = D/50$. The loading platens were allowed to rotate freely in all directions around the loading points at the top and bottom concrete faces. The loading platens were glued to the concrete. Six different sizes were tested; all specimens were geometrically similar (see Fig. 1). The specimen thickness was kept constant ($b = 0.1$ m), implying a transition from plane strain like conditions at the smallest size to plane stress conditions for the large sizes. The concrete mixture was reported to have an average cube compressive strength of 50 MPa and a maximum aggregate size $d_{\max} = 8$ mm.

For comparative purposes, it is necessary to define a nominal strength σ_N. Since the eccentricity of the loading points has been geometrically scaled in both experiments and numerical models, we can ignore its effect on the linear state stress field and define the nominal stress σ simply as a function of the characteristic dimension D (maximum specimen width), instantaneous tensile force F applied at the concrete faces at the eccentricity e and the cross-sectional area in the middle of the specimen A ($=0.6Db = 0.06D$ m^2)

$$\sigma = \frac{F}{A} \tag{1}$$

Having defined the nominal stress, we define the nominal strength σ_N as the nominal stress attained at maximum loading force ($\sigma_N = F_{max}/A$).

Note that the smallest specimen size A has a width in the 'neck-area' of 30 mm. Compared to the maximum aggregate size of 8 mm, it must questioned whether such a small specimen (being too small in size to be considered a representative volume element) can still be treated identically to the rest of the series.

3. The deterministic model

A strong contribution to the nonuniformity of the nominal strength is the "energetic-deterministic" size effect caused by an approximately constant fracture process zone (FPZ) size with stress redistribution in specimens of all sizes (see, e.g., Bažant and Planas, 1998). This effect can be modeled e.g., by the finite element method provided that the fracture energy and the whole shape of pre- and post-peak behavior is correctly introduced. We created the deterministic model in the ATENA software package (Červenka and Pukl, 2005), using Bažant's microplane material model (version 4) (Bažant et al., 2000) and the crack band model (Bažant and Oh, 1983) as a simple regularization. The basic idea of the crack band model for strain-softening in tension (and also of the model of Pietruszczak and Mróz (1981) for strain-softening in shear) is to modify the material parameters controlling the smeared cracking such that the energies dissipated by large and small elements per unit area of the crack band would be identical. The choice of the microplane constitutive model is supported by the fact that M4 seems to be the best model able to capture the complex behavior of concrete under general conditions. The crack band model has been chosen as the only technique widely used and incorporated in commercial codes due to its simplicity. The M4 microplane model does not explicitly work with strain decomposition into elastic and inelastic parts and therefore the so-called equivalent localization element (Červenka et al., 2005) has been implemented into ATENA. This technique removes the problem of the spurious mesh size dependence of the results, while a certain dependence on the mesh orientation still remains (for a concise overview of various numerical methods and their ability to analyse localization and failure in engineering materials, see de Borst et al., 2004).

Specimens were loaded by deformation increments and the force F was monitored, see Fig. 1, right. We ignored the transition from plane strain to plane stress conditions with growing specimen size and modeled the whole series of sizes with a plane stress model. Based on the information about the average cube compressive strength of 50 MPa, ATENA generated a set of consistent microplane parameters: $K1 = 1.5644\text{E}{-}04$, $K2 = 500$, $K3 = 15$, $K4 = 150$ (Caner and Bažant, 2000), crack band $c_b = 30$ mm, number of microplanes 21 (an efficient formula that still yields acceptable accuracy involves 21 microplanes to integrate over a sphere (Bažant and Oh, 1986)). The parameters $K1$ through $K4$ are phenomenological microplane model parameters and they do not have a physical meaning; they can be understood as scaling parameters of given curve shapes (criteria) describing the so-called "boundaries". Briefly, $K1$ plays a role in relations for the tensile normal boundary (needed for tensile cracking, fragment pullout and crack closing), and also compressive deviatoric and tensile deviatoric boundaries (spreading and splitting); $K1$ and $K2$ affect shear boundary (friction); $K1$, $K3$ and $K4$ are present in the relations for both tensile and compressive volumetric boundaries (pore collapse, expansive breakup); for a full description, see Bažant et al., 2000.

We changed the crack band to 8 mm, a value that better matches the experimental data, see Fig. 2, left. The crack band size is related to the fracture energy of the material and controls the size at which the continuum computational model undergoes transition from relatively ductile to elastic-brittle failure (transition between two horizontal asymptotes in the size effect plot, see Fig. 2). A noticeable fact is that in the size effect plot the curve can be shifted right or left as a rigid body just by changing c_b. More specifically, the deterministic nominal strength computed for a certain size of D using a c_b value is also the nominal strength of size s D computed with crack band width sc_b (s is a positive scaling parameter)

$$\text{for } \forall s > 0: \quad \sigma_N^{det}(D, c_b) = \sigma_N^{det}(sD, sc_b) \tag{2}$$

Not only the nominal strength is equal for the scaled structure. If both the structure and crack band width is scaled s times, the stress and displacement fields take the same values over the scaled coordinates. This fact can be exploited to simplify the preprocessing of numerical models of a size effect series: simply create a model of one size only and vary c_b instead of D. For instance, we do not have to model all sizes in ATENA, but modify

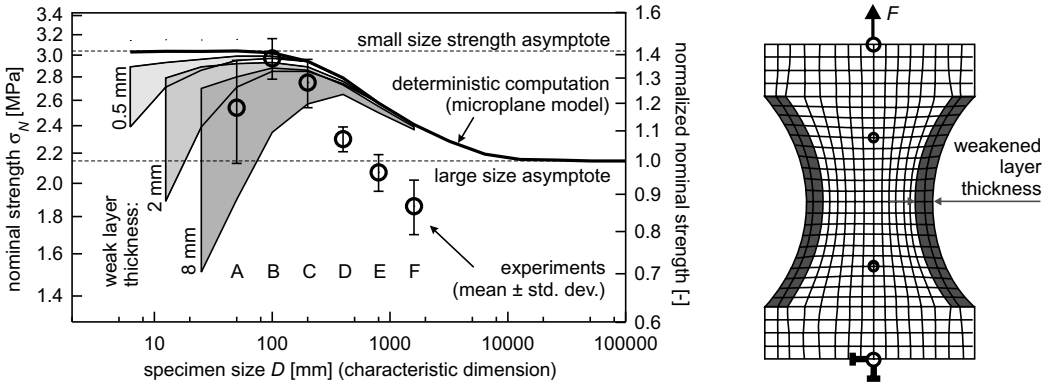

Fig. 2. Left: size effect plot for experimental data by van Vliet and van Mier (1998) compared to 'deterministic' and 'weak layer' computations. Right: computational model with a surface weak layer.

c_b in a single model to obtain the response for another size. This illustrates the scaling properties with c_b standing for the *deterministic length*.

It should not remain unnoticed that Eq. (2) has a direct relation to the Vashy–Buckingham Π-theorem (Vashy, 1892; Buckingham, 1914) on dimensional analysis (see e.g., Barenblatt, 1996). It turns out that, given all parameters, the nominal structural strength depends on the dimensionless ratio of D and c_b. If their ratio is close to unity, the structure is in transition between two important asymptotes: plastic and elastic solutions. More precisely, if the structure is much smaller than c_b ($D/c_b \to 0$), the behavior is fully elasto-plastic and can be simply predicted based on the knowledge of direct tensile strength f_t (the yielding point in this case). On the other hand, if the structural size D is much larger compared to c_b, the behavior is linear elastic with a sudden failure at the onset of reaching the direct tensile strength f_t at any point in the material (see e.g., Vořechovský et al., 2005; Bažant et al., in press). In this case, what matters is the profile of principal tensile stresses over the structure, see Fig. 6, right. From this we can also deduce the value of $\sigma_N^{det}(\infty, c_b)$, it being the large size asymptote in Fig. 2. Simply, it is the nominal stress when the largest principal tension reaches the direct tensile strength f_t. Note that in the definition of σ_N the eccentricity of loading and possible stress concentration in the specimen's neck are not reflected and therefore $f_t \neq \sigma_N^{det}(\infty, c_b)$.

4. Weak boundaries

A plausible hypothesis can be used to explain the strength decrease in small specimens. We believe that, apart from other irregularities (such as the strain distribution including out-of-plane rotations, van Vliet and van Mier, 1999, etc.), the smallest specimen suffers the most from having a surface layer of a material with lower stiffness and strength. As argued in RILEM-TC-QFS (2004) and van Mier (2004), the surface layer of load-free specimens is in tension and undergoes cracking at the beginning of drying. The differential shrinkage and differential temperatures during hardening of the concrete induce eigen-stresses. These eigen-stresses have the most significant effect on the behavior of small specimens due to their large specific area (van Vliet and van Mier, 2000a). In very large specimens however, the cores do not suffer any drying over their entire lifetime. Therefore, the size effect will be much less affected by drying in large specimens compared to small specimens.

A simple way of incorporating the effect of micro-cracking into the model is to reduce the material strength in the surface layer. A parametric study has been performed to illustrate the effect of (i), the weakened surface layer thickness and (ii), the reduction of the material strength in that layer. In Fig. 2, we plot six size effect curves computed with the deterministic model equipped with a layer of weakened material on both curved edges of the specimen (see the illustration on the right). In particular, we selected three thicknesses t_w (0.5, 2 and 8 mm) and for each thickness we considered two different reduction factors for the material strength parameter r_t (0.5 and 0.9). In the figure, two curves are plotted for each layer thickness and the space between them is filled with gray color (the upper curve always corresponds to a reduction of 0.9 and the lower one to a

reduction of 0.5). It can be seen that the nominal strength reduction decays as the layer thickness becomes negligible compared to specimen dimension D. Moreover, the ratio between the reduced strength and the deterministic nominal strength can be roughly used as a strength reduction coefficient for any dimensionless ratio t_w/D. This reveals a simple scaling rule written for an arbitrary positive scaling factor s and the reduction factor r_σ of specimen strength due to the weak strip compared to the deterministic strength with no strip

$$r_\sigma\left(\frac{t_w}{D}\right) = \frac{\sigma_N(D,t_w)}{\sigma_N^{det}(D)} \cong \frac{\sigma_N(sD,st_w)}{\sigma_N^{det}(sD)} \tag{3}$$

$r_\sigma \in \langle r_t; 1\rangle$, where $\sigma_N^{det}(D)$ is the deterministic strength for size D; $\sigma_N(D,t_w)$ is the deterministic strength for size D and weak layer thickness t_w; r_t is the reduction factor for material strength within the weak layer $r_t \in \langle 0; 1\rangle$.

The best results are obtained with $t_w = 2$ mm and reduction coefficient $r_t = 0.5$. As can be seen from Fig. 2, we are able to partly fit the drastic strength reduction in specimens where the thickness t_w is not negligible compared to the specimen neck thickness of $0.6D$. The deterministic size effect studied in the previous section is automatically included in the computation because we use the same material model and parameters. However, the most important effect of strength reduction for large specimens cannot be modeled by the two effects studied so far. Neither are we able to model the strength scatter because randomness has not been considered in the model yet.

5. The stochastic model

We believe that the strong size effect on strength in the experimental data is predominantly caused by the spatial variability/randomness of local material strength. Therefore, we considered the strength related parameter in the microplane model denoted $K1$ in ATENA to be random, and performed Monte Carlo type simulations for each size of specimen. In particular, we sampled 64 random field realizations of the parameter $K1$ for each size and computed the responses (complete σ–Δu diagrams, stress fields, crack patterns, etc.). We tested numerically that parameter $K1$ has an approximately linear relation to structural strength within a wide range around the mean value used in the deterministic model. The reason for sampling the local material strength by random field instead of by independent random variables is that we believe that in reality the strength of any two close locations must be strongly related (correlated) and that such a relationship can be suitably modeled by an autocorrelated random field, see Fig. 3, right. We assumed the distribution of local strength at each material point to be identical and Weibull distributed, see Fig. 3, top-left. The local probability of failure p_f (cumulative distribution function F_σ) depending on stress level σ reads

$$p_f = F_\sigma(\sigma) = 1 - \exp\left[-\left(\frac{\sigma}{\sigma_0}\right)^m\right] \tag{4}$$

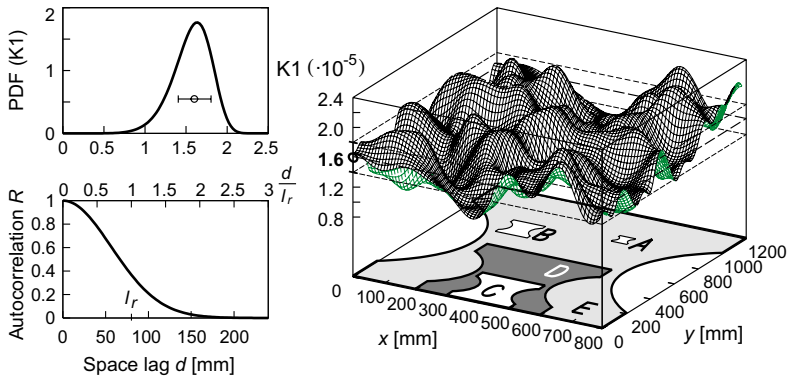

Fig. 3. Top-left: Weibull probability distribution function of the randomized parameter $K1$ (Eq. (4)). Bottom-left: autocorrelation function (Eq. (5)). Right: realization of a Weibull random field of $K1$ compared with dog-bone specimens type A–E. The dashed lines correspond to the mean and mean ± one standard deviation of $K1$.

where σ_0 is the scale parameter of Weibull distribution, a value of 1.6621E−4 MPa used for $K1$; m is the shape parameter of Weibull distribution (dimensionless, depends solely on cov which is the coefficient of variation), $m = 7.91$ being used for random $K1$.

To obtain results consistent with previous deterministic analysis we kept the value of parameter $K1$ as the mean value. The second parameter of Weibull distribution has been set with regard to the cov of the nominal strength of the smallest specimen A (in experiments the cov of strengths of size A was 0.16). This choice is supported by the fact that size A has the largest sample size (10 replications, see Table 1). Therefore, the estimation of variance has a higher statistical significance than for other sizes. Moreover, we believe that the effect of the weakened boundary reduces only the mean nominal strength and does not influence the scatter of strengths. For simplicity, we used the value of cov = 0.15 (15% variability of local material strength). This is a relatively high value implying the unusually low Weibull modulus mentioned above. Note that a different choice of Weibull modulus based e.g., on the scatter of nominal strengths for size C would lead to higher m ($\approx$16) and therefore less scattered results (cov $\approx$ 0.08) and a milder slope in the asymptotic size effect curve for $D \to \infty$. As will be seen later, such a choice would not be consistent with the slope predicted by the average nominal strengths of sizes E and F, which is, again, around $m \approx 7.9$.

On the other hand, the scatter of experimentally obtained peak forces is much higher for size A suggesting that there was a strong influence of additional imperfections in shape, geometry and boundary conditions (eccentricity, etc). As will be seen later, the asymptotic slope of the mean size effect $-1/7.91$ does not equal the value of $-1/6$ suggested by averages of all sizes except size A (and used in a simple Weibull slope fit by van Vliet and van Mier (2000a,b)). In our opinion, the Weibull modulus of 6 is too high. The fact that it matches the averages of sizes B to F means that in that size range the deterministic-energetic size effect also plays a partial role (leading to an pronounced slope in the curve). There are more sources of size effect acting together and the Weibull size effect alone should not be used to mimic all of them. The issue of the correct choice of statistical scatter of the material strength is further discussed in Section 6.

A discretized random field is a set of autocorrelated random variables. The most important parameter (in a given form of autocorrelation function) is the autocorrelation length controlling the distance over which the random material strengths are correlated. We used the squared exponential autocorrelation function (Fig. 3, bottom-left)

$$R = \exp\left[-\left(\frac{d}{l_r}\right)^2\right] \tag{5}$$

where d is the distance between two points; l_r is the correlation length, a value of 80 mm used for a random field of $K1$.

The correlation length l_r is assumed to be a material (and possibly structural) constant related either to the microstructure (grain size and defect distribution and their frequency, i.e., on their distance from each other), and also on the production technique (compacting, etc.). The autocorrelation function takes values close to unity for any two close points in the specimen (unit correlation is the upper limit for two coinciding points). For a pair of remote points the autocorrelation decays to zero implying no statistical correlation for the material properties of those two points. It can be shown that for specimens much smaller than one autocorrelation length, the realization of a random field of the local strength $K1$ is a constant function over the whole region

Table 1
Experimental data

	D (mm)	r 0.725D (mm)	σ_N mean (std. dev.) (MPa)	Specimens tested (#)
A	50	36.25	2.54 (0.41)	10
B	100	72.5	2.97 (0.19)	4
C	200	145	2.75 (0.21)	7
D	400	290	2.30 (0.09)	5
E	800	580	2.07 (0.12)	4
F	1600	1160	1.86 (0.16)	4

Specimens' dimensions, nominal strengths and sample size.

(see Fig. 3, right), and all local strengths of the whole specimen can be represented by just one random variable (instead of a number of spatially correlated variables). Since the specimen's nominal strength is just a simple transformation of the input strength parameter $K1$ (no spatial variability, allowing cracks to localize in other locations than in deterministic analysis), we knew that the mean nominal strength of the smallest specimen will be the same as that obtained by deterministic analysis. That is why we used the $K1$ from deterministic analysis as the mean value of the random field of $K1$.

The samples of random fields evaluated at the locations of integration points were simulated by methods described in Vořechovský (in review, 2004b) and Vořechovský and Novák (2005). In the method, the support of the field is discretized (nodes of the random field mesh may coincide directly with the integration points of the FEM mesh). Based on the discretization and a given autocorrelation function (Eq. (5)) an autocorrelation matrix $\boldsymbol{C}$ is assembled. Such a matrix is symmetric and positive definite and has orthogonal eigenvectors $\boldsymbol{\Phi}$ and associated eigenvalues $\boldsymbol{\Lambda}$ such that $\boldsymbol{C} = \boldsymbol{\Phi}\boldsymbol{\Lambda}\boldsymbol{\Phi}^{\mathrm{T}}$. The (discretized) Gaussian random field $\boldsymbol{X}$ is expanded using a Gaussian random vector $\boldsymbol{\xi}$ and the computed eigenmodes as $\boldsymbol{X} = \boldsymbol{\Phi}(\boldsymbol{\Lambda})^{1/2}\boldsymbol{\xi}$. If nonGaussian fields are to be simulated, the Nataf model is usually employed (Liu and Der Kiureghian, 1986). The simulated random fields are stationary, isotropic and homogeneous. Briefly, the described orthogonal transformation of the covariance matrix has been used in combination with Latin Hypercube Sampling of the random part of field expansion (Novák et al., 2000). Such a combination proved itself to be very effective in providing samples of random fields leading to high accuracy in estimated response statistics compared to classical Monte Carlo sampling. Numerical studies documenting this efficiency are published in (Vořechovský, in review, 2004b; Vořechovský and Novák, 2005). This is an extremely important property in cases when the evaluation of each response is very time consuming. In our case the evaluation is represented by one computation of response by the nonlinear finite element method with the microplane material model inside. Obviously, this is very expensive and we must keep the number of simulations as low as possible. The number of 64 simulations was tested to be high enough and to provide stable and accurate statistical estimates of fields' statistics (averages, sample standard deviations, autocorrelation structure) as well as reproducible estimates of structural response statistics (nominal strength, etc.).

The automatic simulation of all structural responses was done by SARA software integrating (i) ATENA software (evaluation of response) and (ii) FREET software (Vořechovský, 2004b; Novák et al., 2006; Novák et al., 2003b) (simulation of samples of random parameters, statistical assessment).

In Fig. 4, we plot computed sets of 'nominal stress–displacement' (σ–Δu) diagrams and sketch the definition of displacement (the separation of two measuring points). The diagrams are plotted only for specimen sizes C–F, because the diagrams of sizes A, B look similar to that of size C. Selected load displacement curves are highlighted and the corresponding realizations of random strength fields are plotted in Fig. 5. The letter denotes specimen size and the integer denotes the number of the simulation. Besides the most frequent simple σ–Δu functions we have purposely highlighted several curves with unusual shapes (snap-back type or "a loop"). When testing concrete structures in routine practice such special shapes can only occasionally be experimentally measured. They would indicate that the control length was not properly designed (with respect to the specimen shape and material strength variability) and that localized strains occur outside the control length. As discussed later, in our case some unusual or unexpected curves were obtained partly due to the definition of displacement Δu, and mainly due to the spatial randomness with a high variability. A comparison of the peak strength of the deterministic σ–Δu diagram with the mean value of nominal strength can be made in Fig. 4. The difference between them grows with specimen size. While for size C the mean strength nearly coincides with the peak of the deterministic diagram, for specimen size E the deterministic curve is above all 64 random realizations of the diagram, see Fig. 4.

In Fig. 5, we plot chosen realizations of the random strength field for all sizes A–F. We note that a similar scaling rule as in Eq. (2) can be written for the role of statistical length (here in the form of autocorrelation length l_{r}). For a given random strength field (statistical distribution and autocorrelation structure) only the dimensionless proportion D/l_{r} matters (recall the dimensional analysis)

$$\text{for } \forall s > 0: \quad \sigma_{\mathrm{N}}(D, l_{\mathrm{r}}) = \sigma_{\mathrm{N}}(sD, sl_{\mathrm{r}}) \tag{6}$$

Again, this can be used to simplify modeling because one size can be used with varying l_{r} instead of D. Similarly to Eq. (2), this property illustrates the scaling properties with l_{r} standing for a *probabilistic* (or *statistical*)

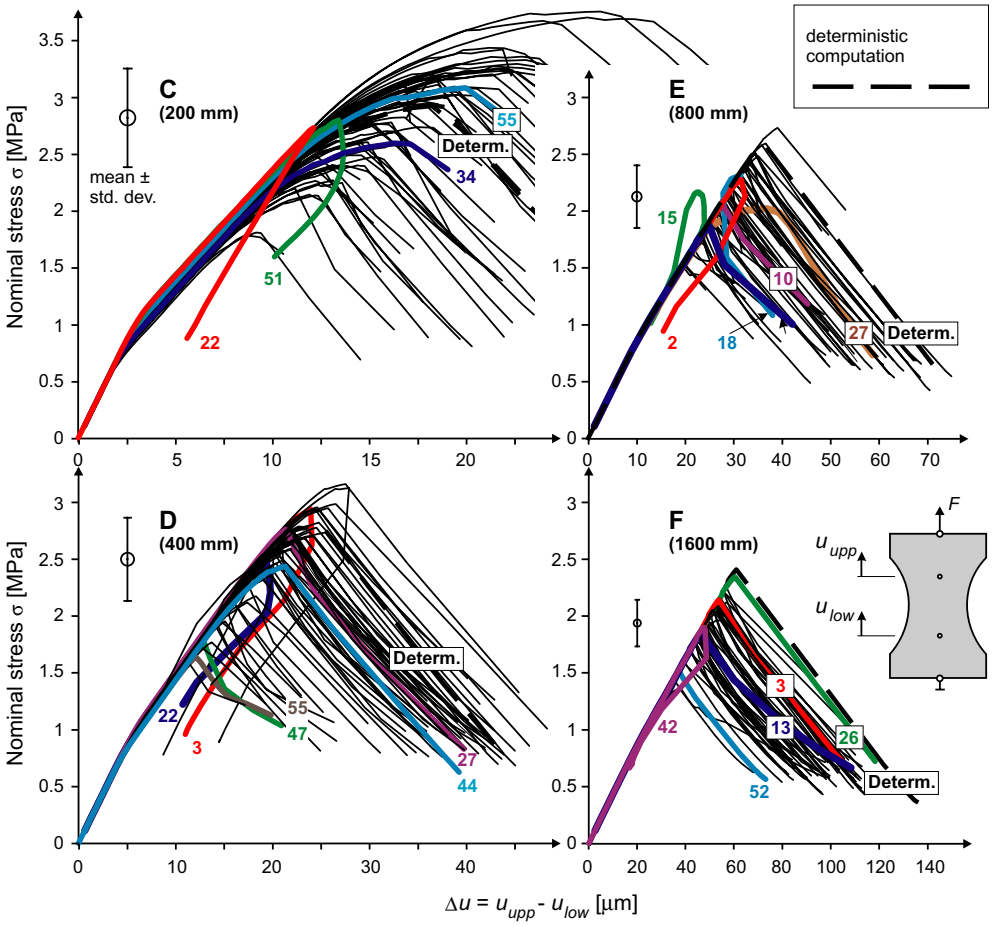

Fig. 4. Nominal stress–displacement diagrams (64 realizations) of structural sizes C, D, E and F. Selected diagrams are highlighted.

scaling length. Similarly as with the deterministic size effect caused by stress redistribution in FPZ, the probabilistic size effect curve represents a transition between two asymptotes (horizontal for $D \to 0$ and an inclined straight line for $D \to \infty$). The transition happens when the nondimensional size D/l_r takes values approximately between 0.1 and 10. An analytical formula for the size effect on strength based on the extremes of random fields has been formulated by Vořechovský (2004a,b) and used to predict the strength of thin fibers (Vořechovský and Chudoba, 2006) or in the context of the energetic-statistical size effect in quasibrittle structures failing after crack initiation (see Vořechovský et al., 2005; Bažant et al., in press).

It can be seen that as the ratio of autocorrelation length and specimen size D decreases, the rate of spatial fluctuation of random field realizations grows. Therefore, there are an increasing number of locations with low material strength (locations prone to failure). Or, in other words, with increasing specimen size there is an increased probability that there will be a weak spot in highly stressed regions. This effect has long been referred to as the statistical size effect. The classical statistical size effect is modeled by the simple weakest link model and is usually approximated by the Weibull power law (Weibull, 1939). However, as explained in (Vořechovský, 2004b,a; Vořechovský and Chudoba, 2006), the classical Weibull model is not able to account for spatial correlation between local material strengths. Rather, the Weibull model is based on IID (independent and identically distributed) random variables linked in series. The effect of such a consideration is that the strength of an infinitely small specimen is infinite. In the Weibull model every structure is equivalent to a chain under uniaxial tension, a chain of independent members having an identical statistical distribution of stress. If the local strength is modeled by an autocorrelated random field (and we consider the autocorrelation length to be a material property), the small size asymptote of strength is equivalent to the distribution of local material

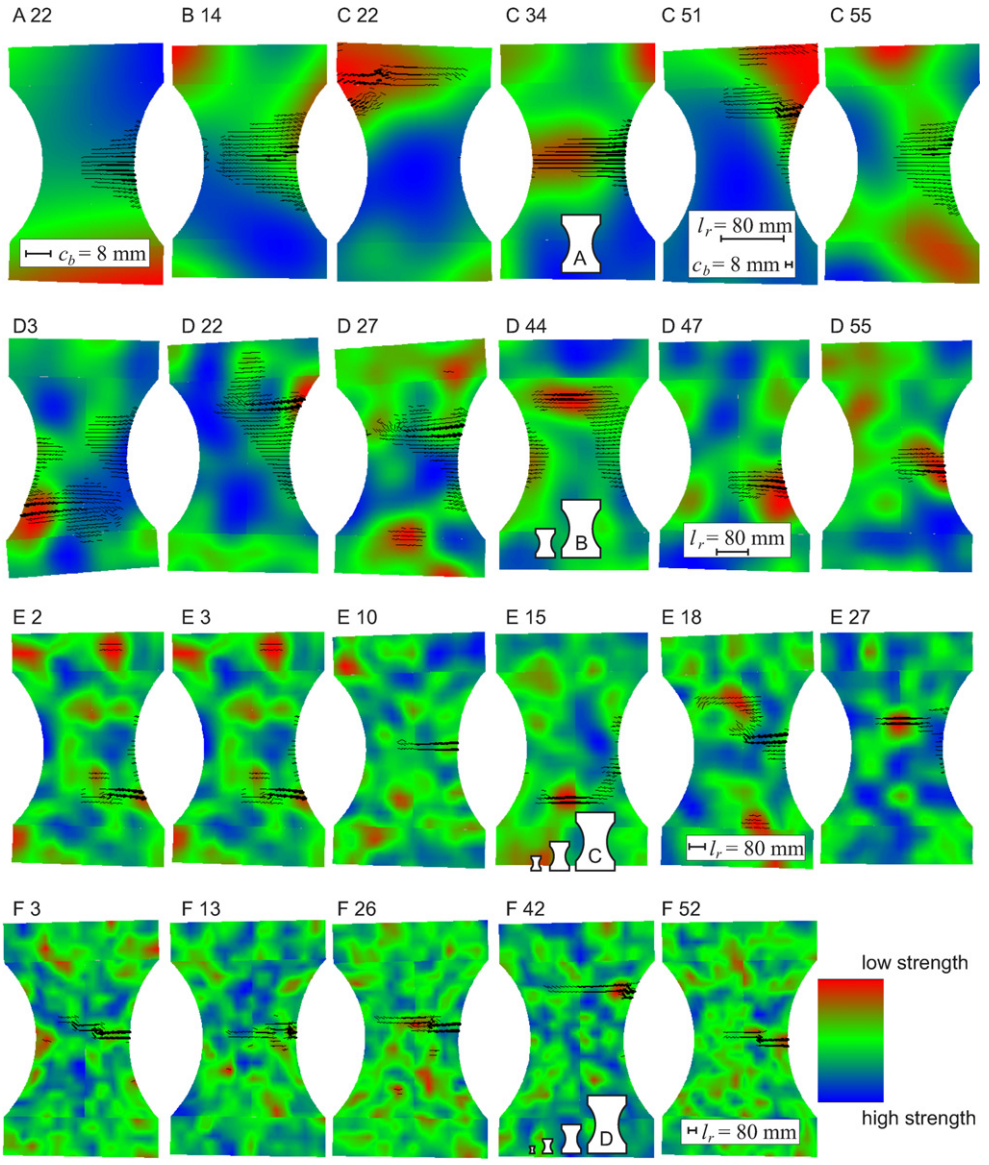

Fig. 5. Simulated random strength field realizations and corresponding crack patterns in deformed specimens right after attaining the maximum force F_{max}. Fields were simulated and crack widths were computed at the integration points of finite elements.

strength. On the other hand, the large size asymptote is exactly identical to that of the Weibull model (for a proper choice of reference length and the corresponding scale parameter of Weibull distribution in the Weibull model). The autocorrelation length plays an important role as a statistical scaling length in a material controlling the transition from a one strength random variable model (full correlation in small structures) to many independent local strengths (large structures, Weibull model) (see Vořechovský, 2004a,b) for details.

The crack patterns of two randomly chosen specimens A 22 and B 14 (see Fig. 5) show the most frequent location of strain localization. The small eccentricity of load and relatively narrow neck of dog bone specimens nearly guarantee that cracking will initiate on the right side of the neck. Samples of random fields in both cases (A, B) are nearly constant functions and therefore there is no space left for the weakest link principle. Pattern C 22 in the same figure documents that the local strength can be, in some locations, so small that the relatively low stresses in that location can initiate fracturing. In specimen C 22 the rotation of platens was opposite to the usual direction. Since the damage localized out of the distance at which we measured the displacement Δu,

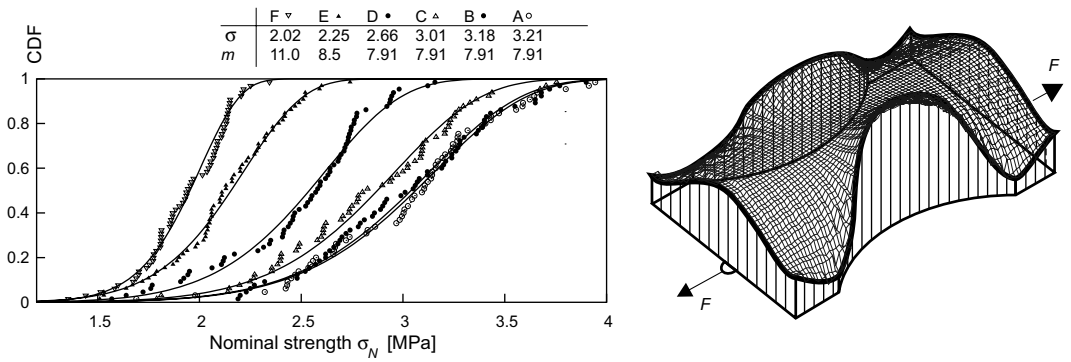

Fig. 6. Left: estimated distribution of the nominal strengths of specimens with a random Weibull field of $K1$. Best fits by Weibull distribution (Eq. (4)). Right: computed field of principal tension over the specimen in an elastic stress state.

the corresponding σ–Δu diagram in Fig. 4 has the snap-back-like shape. The fact that the specimen breaks in the relatively low stressed region is associated with the relatively high variability of local material strength. Simply, the realization of the strength field in the cracked region was the closest to the principal tensile stress profile, see Fig. 6. If a different strength distribution was chosen (especially lower variability), the occurrence of fracturing outside the neck area would be suppressed. The same is true also for C 51 whereas C 34 and C 55 are again just typical representatives of σ–Δu diagrams and crack patterns. Similar features can be found in series D. The positions of cracking in D 3 and D 22 caused the snap-back-like shapes while D 27, D 44, D 47 and D 55 illustrate the random sampling of crack initiation leading to the usual shape of the σ–Δu diagram displayed on our virtual testing machine.

Very interesting are diagrams E 15 and E 18. The ''loops'' in Fig. 4 are the results of an unfortunate case of cracking close to the points of measured displacement. It can happen that at some point of loading the lower measuring point can start moving faster than the upper point and this results in a bizarre shape of σ–Δu as in diagram E 15. A specimen can later start cracking in the neck as occurred in the case of E 18. In series F the autocorrelation length becomes so small compared to specimen dimension that again cracks initiate on the right side of the neck in nearly all cases, see Figs. 4 and 5. In series A, we never reported a snap-back-like curve due to cracking outside the measuring distance, and in the cases of B and F this happened once only, see Fig. 4. We can conclude that the most interesting processes happen in specimens with a dimension comparable to one or two correlation lengths (region of transition from one random strength variable to a set of independent strength variables).

We note that in contrast to the experiments, we did not control loading by displacement increments Δu. Instead, we loaded the specimens by displacement at the ends, and therefore we were able to monitor the snap-back type of curves without any difficulty.

5.1. The Weibull integral

We were able to simulate the random responses of specimens even smaller than A with random fields of $K1$, and moreover we could simply use random variable sampling to represent randomness in the small specimens (each realization becomes a random constant function over the specimen). On the other hand, it becomes very problematic to simulate samples of random fields of specimens much larger than F. Approaches already exist to overcome the computational difficulties with the stochastic finite element computation of large structures (Vořechovský et al., 2006) but we will present another technique here. Fortunately, only strength is random in our analysis and we can use the classical Weibull integral for large structures. As explained in (Vořechovský, 2004b,a; Vořechovský and Chudoba, 2006), if the structure is sufficiently large, the spatial correlation of local strengths becomes unimportant and the Weibull integral yields a solution equivalent to a full stochastic finite element simulation. We will briefly sketch the computational procedure of evaluating the Weibull integral for

structural failure probability: details can be found e.g., in (Bažant and Planas, 1998). The Weibull integral has the form

$$-\ln(1-P_{\mathrm{f}}) = \int_V c[\sigma(\mathbf{x}); m, \sigma_0]\,\mathrm{d}V(\mathbf{x}) \tag{7}$$

where P_{f} is the probability (the cumulative probability density) of failure load of the structure; $c[\bullet]$ is the stress concentration function.

There are several possible definitions of the stress concentration function, see Bažant and Planas (1998). In the studied specimens the major contributor to the stress tensor is the normal stress σ_{yy}. The field of stress σ_{yy} nearly coincides with the principal tension σ_I. Since only tensile stresses are assumed to cause a failure, we defined the stress concentration function simply as

$$c[\sigma(\mathbf{x}); m, \sigma_0] = \frac{1}{V_0}\left\langle \frac{\sigma_I(\mathbf{x})}{\sigma_0} \right\rangle^m \tag{8}$$

where V_0 is the reference volume associated with m and σ_0.

In Fig. 6, right, we plot a computed field of principal tension over a specimen in an elastic stress state. Numerical integration of this stress field for different specimen sizes and failure probabilities can be suitably rewritten in dimensionless coordinates so that the computation becomes extremely easy. The resulting mean size effect is plotted in Fig. 7 (asymptotic mean size effect curve). Let us also mention that another way of simulating the random strength of large structures can be done utilizing the stability postulate of extreme values (Fisher and Tippett, 1928). Such a computational procedure is an elegant trick using the recursive property of the distribution function and is described in Bažant et al. (in press), Novák et al. (2003a) and Vořechovský (2004b) together with applications. The results of such an approach (and also the Weibull integral as presented here) are valid only for extremely large sizes where the effects of structural nonlinearity (causing stress redistribution) disappear. For small sizes there are two problems: (i) the spatial correlation of local strengths and (ii) the effect of stress redistribution. The result must be a straight line in a double logarithmic plot of size versus strength (the size effect plot is a power law). An approach based on the simple scaling of Weibull random variables associated with structural regions of different sizes has been used in Lehký and Novák (2002). They simply used the scaling rules only for sizes larger than size C, and this helped them to obtain a close fit of

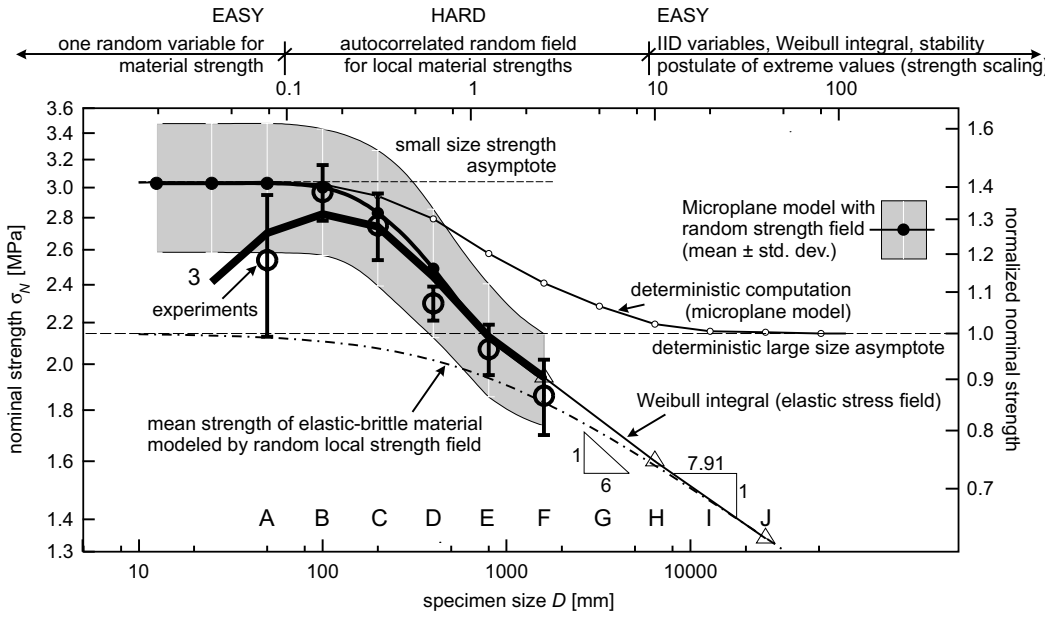

Fig. 7. Comparison of results in a size effect plot.

experimental data. Unfortunately, the numerical model used did not allow platens to rotate freely and did not model the eccentricity of loading force, and both of these factors, in our view, can negatively affect the results of response statistics. By prescribing both platens to move without rotation one forces the specimen to fracture differently than if platens can rotate freely. This becomes extremely important if the local strength becomes randomized spatially.

5.2. Comments on local and nonlocal Weibull theories

The probability P_f of failure of a quasibrittle structure is realistically approximated by nonlocal generalization of the Weibull statistical theory (developed in Bažant and Xi (1991) and refined in Bažant and Novák (2000)). The nonlocal Weibull integral has the same form as the local one (Eq. (7)) except for the choice of stress concentration function $c[\sigma(\mathbf{x}); m, \sigma_0]$. While the local integral directly uses the stress field $\sigma(\mathbf{x})$ without any modification, the nonlocal version uses the 'nonlocal stresses' $\overline{\sigma}(\mathbf{x})$. There are several ways to obtain $\overline{\sigma}(\mathbf{x})$ (see, e.g., Bažant and Planas, 1998). The most frequently used is the averaging of inelastic strains that are used to compute $\overline{\sigma}(\mathbf{x})$. The important feature is that strains undergo averaging with a certain weight function $\alpha(\mathbf{x},\mathbf{s})$ (e.g., a bell-shaped function) over a nonlocal characteristic volume Ω centered at point $\mathbf{x}$. For a given shape of the weight function, the nonlocal volume (area, length) is driven by a characteristic length ℓ (similar to the autocorrelation length l_r) which then represents a material property related e.g., to maximum aggregate size.

The physical cause of the energetic part of size effect (influenced by the characteristic length c_b in the crack band model or ℓ in nonlocal models), is the stress redistribution and energy release caused by a sizable boundary layer of cracking (or FPZ) and microcrack interactions, and the length is set principally by the material inhomogeneity size, i.e., the aggregate size in concrete. On the other hand, the physical cause of the statistical part of size effect is mainly the randomness of material strength. The nonlocal Weibull theory uses the same length ℓ for both sources and in a way overcomes the problem of the lack of spatial correlation in local Weibull theory via the sliding average.

The averaging in Eqs. (7) and (8) cannot, of course, introduce a length scale for a body under uniform stress, in which case other, purely statistical, length scales may arise due to autocorrelation. On the other hand, it has been demonstrated by asymptotic analysis as well as numerical simulations that, for large enough structures ($D \to \infty$), the nonlocal Weibull theory reduces to the classical (local) Weibull statistical theory, for which $\overline{\sigma}(\mathbf{x})$ in Eq. (7) is replaced by local stress $\sigma(\mathbf{x})$. There is no characteristic material length in the classical (local) theory, because the Weibull size effect is self-similar – a power law with no characteristic length and no upper bound. Rather, l_r (or V_0) in Weibull theory is simply a chosen unit of measurement to which the spatial density of failure probability is referred.

Because the statistical and energetic physical causes of size effect are different and independent, l_r cannot be affected by changes in c_b. The nominal strength σ_N must be bounded when $D \to 0$, (i.e., the statistical size effect cannot cause a strength increase when the structure is too small as in the classical Weibull theory). Also, the upper bound of the statistical part of size effect is based on the distribution of extremes (minima) of random fields representing local material strength (Vořechovský, 2004b; Vořechovský and Chudoba, 2006).

6. Analysis of the results

By introducing three different scaling lengths we are able to independently incorporate three different effects in the model resulting in three size effects on nominal strength. The crack band width c_b (deterministic scaling length) controls at which size the transition from ductile to elastic-brittle model behavior takes place, and therefore it controls the transition between two horizontal asymptotes in the size effect plot (see Fig. 2). The second introduced length (weak boundary thickness, t_w) together with material strength reduction controls at which size there will be a significant reduction in nominal strength. The reduction becomes amplified with decreasing specimen size and causes an opposite slope of size effect than with the deterministic and statistical ones (see Fig. 2). The last introduced length is the autocorrelation length l_r controlling the transition from randomness caused by overall material strength scatter (one random variable for material strength) to a set of independent identically distributed random variables of local material strengths via an autocorrelated

random field. In other words, it controls the convergence to the Weibull statistical size effect based on the weakest link principle. Such an interplay of three independent material/structural lengths is very complex. It would be nearly impossible to determine all these parameters from the available experimental data even if the model featuring the three effects was perfectly correct.

In Fig. 6, left, we plot the estimated distribution function of nominal strength for all tested sizes as we obtained them from the full stochastic finite element analysis with the parameter $K1$ modeled by random field. The table above the graphs presents the parameters of Weibull distribution that best fit the empirical histograms. For some reason it happened that the Weibull modulus increased for sizes E and F even if the slope of the corresponding size effect curve in Fig. 7 again suggested the value 7.91 (the value that we expected and that follows from the simple Weibull size effect of an elastic-brittle structure). The deviations may have been caused by numerical errors; especially, insufficient discretization of the random field with respect to the autocorrelation length. The variability is not captured sufficiently by the density of integration points because we did not increase the mesh density for models of large specimens. Rather, we kept the same number of finite elements for all sizes in order to save computational time.

The resulting nominal strengths for all sizes obtained by nonlinear stochastic FEM are plotted and compared to experiments in Fig. 7. We see that starting from size C the size dependence on mean nominal strength is *predominantly statistical*, and we were not able to model it by deterministic model alone (see, e.g., Novák et al., 2001). We also included mean nominal strengths for sizes F, H and J obtained by Weibull integral (Eqs. (7) and (8)). The Weibull solution is a straight line and represents the asymptotic size effect of structures caused solely by spatial strength randomness. Above the plots, we sketch the size regions for different computational techniques used for the modeling of random strength.

The very thick curve in Fig. 7 (denoted as 3) is the curve resulting from the combination of all three effects described here. The curve has been obtained by applying the dimensionless reduction factor r_σ, due to the weak strip, to results obtained by nonlinear stochastic FEM (layer thickness $t_w = 2$ mm, reduction $r_t = 0.5$). This was a simple solution to estimate the final results of a model featuring all effects. Unfortunately this simple approach is not correct because it applies the reduction of the weak layer to the final mean of all the results of simulation with random fields. Generally this cannot be done because the sources of size effect interact. To get a consistent result, one should model the local strengths by random field and apply the reduction in the layer to each realization of a field. This would help the specimens to initiate cracks in their surface layers more often. Unfortunately, a full set of time consuming simulations would be necessary. One can immediately see that the strength of size A is not reproduced correctly (even though the scatter is). We believe that this can partly be improved by considering the plane strain conditions, and most importantly, the fact that the specimen thickness b (=0.1 m) is larger than the width of the specimen, and that in the 3D model the crack would often initiate from the front or back surfaces of the specimen (see illustration in Fig. 1, left). This effect certainly results in a strength decrease for specimen A.

The authors of the experiments have reported that due to the casting of the specimens, the front layers have different material properties than the back layers. We tried to reproduce these effects in 3D models with some success, but the results are beyond the scope of this paper and 3D effects are not covered in this study. van Vliet and van Mier (1999) have shown that the nominal strength drop for the smallest size can nearly entirely be explained by strain/stress gradients that can develop due to the specimen's shape, eccentricity of the external load, material inhomogeneity and eigen-stresses due to differential shrinkage. They performed a thorough study using a linear model in which the considered normal stresses due to (i) tension (with a stress concentration factor corresponding to the dog-bone shape), (ii) bending moment due to the in-plane eccentricity and (iii) the out-of-plane bending moment caused by different stiffness in the casting and mould sides. They actually showed that most of the observed size effect could be explained with such a model. It may suggest that if a full three-dimensional model covering the nonuniformity of stiffness due to casting was used in our analysis, the identified Weibull modulus would be considerably greater. Combining the effect of strain gradients with the weak layer model should be able to fully represent the nominal strength drop for size A. On the other hand, the large sizes may be fitted well by such a model even with reduced material strength variability. The asymptotic slope of statistical size effect ($-1/m = -1/7.91$) is in good agreement with the scatter of measured nominal strengths for size A. However, the m does not correspond to the experimentally observed scatter of sizes B to F (m values deduced from the scatter for those sizes would equal 19.3, 16.1, 32, 21.4 and 14.2, respectively).

Numerical simulations with a lattice model performed by van Vliet (2000) revealed that if a large grain is present in the surface layer of the specimen, the peak load can decrease considerably. Such a mechanism certainly contributes to the increased statistical scatter of nominal strengths in specimen type A. It seems that the mean size effect as well as the statistical scatter at the same time could be explained by a combination of the 'weak layer', 'deterministic-energetic', 'strain gradient' and 'statistical' size effects together. However, a computational study showing this would require a randomized 3D nonlinear model.

In our study the correlation length l_r has been set to a value nearly equal to the thickness of a specimen. At this length, the variation of local strength is just becoming significant and may distort the results for very small specimens.

It must be questioned whether the crack band width is the correct parameter to represent the deterministic scaling length. The softening adjusted modulus of a material point was designed so that a crack band occupying one band of an element's width always dissipates the same amount of energy irrespective of the band width. Unfortunately, we are not able to model a situation where the deterministic characteristic length is greater that the statistical one (represented by the autocorrelation length in our model). This is because we cannot represent a real crack below the level of resolution of FEM discretization.

Moreover, the crack band model is not suitable when more that one crack appears in parallel, because it was primarily designed to correctly represent a single crack passing through a specimen without mesh size dependency. In our simulations it sometimes happened that at the onset of cracking the crack pattern was diffused, and the consumed energy was then probably higher than what was thought to be correct. Fortunately, localization always started soon (in terms of position on the σ–Δu diagram) and the peak force we recorded was not influenced much. In our constitutive model the crack returns energy during unloading, and this supports the hypothesis that the virtual error was not high.

Both the aforementioned issues can probably be solved by using a better regularization technique to prevent spurious mesh localization; the nonlocal continuum model proposed by Pijaudier-Cabot and Bažant (1987). In this model the deterministic length is well defined by the averaging length l_a (internal length of the nonlocal continuum) over which a certain variable is averaged (based on the weight function α) (Jirásek, 1998). In our eyes such a model would better represent the effect of interaction of the two lengths: deterministic l_a and statistical l_ρ. Another very promising option seems to be the cohesive segments method (Remmers et al., 2003) in which the cohesive segments are inserted into finite elements as discontinuities in the displacement field by exploiting the partition-of-unity property of the shape functions.

7. Conclusions

We present a combination of nonlinear computational mechanics tools with a simulation of random fields of spatially correlated material properties in a single platform as an approach to the modeling of failure in quasibrittle materials. The performed numerical simulations of the random responses of tensile tests with dog-bone specimens with rotating boundary conditions performed by van Vliet and van Mier are in good agreement with the published data. Based on the comparison of trends of nominal strength dependency on structural size we conclude that the suggested numerical model featuring three scaling lengths is capable of capturing the most important mechanisms of failure. In particular, we have shown that a portion of the experimentally obtained size effect can be captured at a deterministic level with the help of deterministic length represented by crack band width in our model. Secondly, further strength dependence on size in large specimens is modeled by an autocorrelated random strength field. The important statistical length scale is introduced in the form of the autocorrelation length of the field. It is shown that the inhomogeneity of material properties over the structure in the form of an autocorrelated random strength field gives rise to imperfections that trigger fracturing in highly stressed regions of a structure. The asymptotic size effect form caused by random strength is the classical Weibull power law. By random sampling of the local strength field we were also able to model the random scatter of resulting nominal strengths. The last effect presented here is the weak boundary layer of constant width. This weakened layer results in a reduction in the strength of small specimens which contrasts with the trends of the two previous size effects. The asymptotic properties of all sources and their combinations are given. Also, simple scaling rules, anchored in theoretical dimensional analysis, are suggested. In such a model a complex interplay of three scaling lengths is captured at a time.

Numerical simulations of localization phenomena demonstrate that the introduction of the stochastic distribution of material properties reveal phenomena that would otherwise remain unnoticed. The presented study also documents the well known fact that an experimental determination of material parameters (needed for the rational and safe design of structures) is very difficult for quasibrittle materials such as concrete.

Acknowledgements

This outcome has been achieved with the financial support of the Grant agency of the Czech Republic under project No. 103/06/P086. The author thanks Mr. Sadílek for help with extensive numerical simulations of dog-bone specimens, and also to Prof. Jirásek and Dr. Grassl for the stimulating discussion at the EURO-C'06 conference where the majority of this work was presented.

References

Barenblatt, G.I., 1996. Scaling, Self-similarity, and Intermediate AsymptoticsNo. 14 in Cambridge Texts in Applied Mathematics. Cambridge University Press, Cambridge.

Bažant, Z.P., Novák, D., 2000. Probabilistic nonlocal theory for quasi-brittle fracture initiation and size effect I: Theory. Journal of Engineering Mechanics, ASCE 126 (2), 166–174.

Bažant, Z.P., Oh, B.-H., 1983. Crack band theory for fracture of concrete. Materials and Structures 16, 155–177.

Bažant, Z.P., Oh, B.-H., 1986. Efficient numerical integration on the surface of a sphere. Zeitschrift für angewandte Mathematik und Mechanik (ZAMM), Berlin 66 (1), 37–49.

Bažant, Z.P., Planas, J., 1998. Fracture and Size Effect in Concrete and Other Quasibrittle Materials. CRC Press, Boca Raton and London.

Bažant, Z.P., Xi, Y., 1991. Statistical size effect in quasibrittle structures. II. Nonlocal theory. Journal of Engineering Mechanics, ASCE 117 (11), 2623–2640.

Bažant, Z.P., Caner, F.C., Carol, I., Adley, M.D., Akers, S.A., 2000. Microplane model M4 for concrete. I: Formulation with work-conjugate deviatoric stress. Journal of Engineering Mechanics, ASCE 126 (9), 944–961.

Bažant, Z.P., Vořechovský, M., Novák, D., in press. Asymptotic prediction of energetic-statistical size effect from deterministic finite element solutions. Journal of Engineering Mechanics, ASCE.

Buckingham, E., 1914. On physically similar systems; illustrations of the use of dimensional equations. Physical Review 4 (4), 345–376.

Caner, F.C., Bažant, Z.P., 2000. Microplane model M4 for concrete. II: Algorithm and calibration. Journal of Engineering Mechanics, ASCE 126 (9), 954–961.

Carmeliet, J., de Borst, R., 1995. Stochastic approaches for damage evolution in standard and non-standard continua. International Journal of Solids and Structures 32 (8–9), 1149–1160.

Carmeliet, J., Hens, H., 1994. Probabilistic nonlocal damage model for continua with random field properties. Journal of Engineering Mechanics, ASCE 120 (10), 2013–2027.

Červenka, V., Pukl, R., 2005. Atena program documentation. Technical report, Červenka Consulting, Prague, Czech Republic. Available from: <http://www.cervenka.cz>.

Červenka, J., Bažant, Z.P., Wierer, M., 2005. Equivalent localization element for crack band approach to mesh-sensitivity in microplane model. International Journal for Numerical Methods in Engineering 62 (5), 700–726.

de Borst, R., Gutiérrez, M.A., Wells, G.N., Remmers, J.J.C., Askes, H., 2004. Cohesive-zone models, higher-order continuum theories and reliability methods for computational failure analysis. International Journal for Numerical Methods in Engineering 60 (1), 289–315.

Dyskin, A., van Vliet, M., van Mier, J., 2001. Size effect in tensile strength caused by stress fluctuations. International Journal of Fracture 108, 43–61.

Fisher, R.A., Tippett, L.H.C., 1928. Limiting forms of the frequency distribution of the largest and smallest member of a sample. Proceedings, Cambridge Philosophical Society 24, pp. 180–190.

Gutiérrez, M.A., 2006. Size sensitivity for the reliability index in stochastic finite element analysis of damage. International Journal of Fracture 137 (1–4), 109–120.

Gutiérrez, M.A., de Borst, R., 2002. Deterministic and probabilistic material length-scales and their role in size-effect phenomena. In: Corotis, R., Schuëller, G., Shinozuka, M. (Eds.), Structural Safety and Reliability: Proceedings of the Eighth International Conference on Structural Safety and Reliability ICoSSaR'01. A.A.Balkema Publishers, Netherlands; Swets & Zeitinger, Newport Beach, California, USA, pp. 129–136.

Jirásek, M., 1998. Nonlocal models for damage and fracture: comparison of approaches. International Journal of Solids and Structures 35 (31–32), 4133–4145.

Lehký, D., Novák, D., 2002. Nonlinear fracture mechanics modeling of size effect in concrete under uniaxial tension. In: Schießl, P. (Ed.), 4th International Ph.D. Symposium in Civil Engineering, vol. 2. Millpress, Rotterdam, Munich, Germany, pp. 410–417.

Liu, P., Der Kiureghian, A., 1986. Multivariate distribution models with prescribed marginals and covariances. Probabilistic Engineering Mechanics 1 (2), 105–111.

Mazars, J., Pijaudier-Cabot, G., Saouridis, C., 1991. Size effect and continuous damage in cementious materials. International Journal of Fracture 51, 159–173.

Novák, D., Lawanwisut, W., Bucher, C., 2000. Simulation of random fields based on orthogonal transformation of covariance matrix and latin hypercube sampling. In: Schuëller, G.I., Spanos Der Kiureghian, P.D., Pestana, M. (Eds.), International Conference on Monte Carlo Simulation MC 2000. Swets & Zeitlinger, Lisse (2001), Monaco, Monte Carlo, pp. 129–136.

Novák, D., Vořechovský, M., Pukl, R., Červenka, V., 2001. Statistical nonlinear analysis – size effect of concrete beams. In: de Borst, R., Mazars, J., Pijaudier-Cabot, G., van Mier, J.G.M. (Eds.), 4th International Conference FraMCoS – Fracture Mechanics of Concrete and Concrete Structures. Swets & Zeitlinger, Lisse, Cachan, France, pp. 823–830.

Novák, D., Bažant, Z.P., Vořechovský, M., 2003a. Computational modeling of statistical size effect in quasibrittle structures. In: Kiureghian, D., Pestana, Madanat (Eds.), ICASP 9, International Conference on Applications of Statistics and Probability in Civil Engineering. Millpress, Rotterdam, San Francisco, USA, pp. 621–628.

Novák, D., Vořechovský, M., Rusina, R., 2003b. Small-sample probabilistic assessment – FREeT software. In: Kiureghian, D., Pestana, Madanat (Eds.), ICASP 9, International Conference on Applications of Statistics and Probability in Civil Engineering. Millpress, Rotterdam, San Francisco, USA, pp. 91–96.

Novák, D., Vořechovský, M., Rusina, 2006. FREeT – feasible reliability engineering efficient tool. Technical Report, Institute of Engineering Mechanics, Faculty of Civil Engineering, Brno University of Technology, user's and theory guides, Program documentation. Available from: <http://www.freet.cz>.

Pietruszczak, S., Mróz, Z., 1981. Finite element analysis of deformation of strain softening materials. International Journal for Numerical Methods in Engineering 17, 327–334.

Pijaudier-Cabot, G., Bažant, Z.P., 1987. Nonlocal damage theory. Journal of Engineering Mechanics, ASCE 113, 1512–1533.

Remmers, R.J.C., de Borst, R., Needleman, A., 2003. A cohesive segments method for the simulation of crack growth. Computational Mechanics 31 (1–2), 69–77.

RILEM-TC-QFS, 2004. Quasibrittle fracture scaling and size effect. Materials and Structures (RILEM Publications SARL) 37 (272), 547–568.

van Mier, J., 2004. Reality behind fictitious cracks? (key-note paper). In: Li, V., Leung, C., Willam, K., Billington, S. (Eds.), 5th International Conference on Fracture of Concrete and Concrete Structures (FraMCoS-V). IA-FraMCoS, Vail, CO, pp. 11–30.

van Mier, J., van Vliet, M., 2003. Influence of microstructure of concrete on size/scale effects in tensile fracture. Engineering Fracture Mechanics 70, 2281–2306.

van Vliet, M., 2000. Size effect in tensile fracture of concrete and rock. Ph.D. thesis, Delft University of Technology, Delft, The Netherlands.

van Vliet, M., van Mier, J., 1998. Experimental investigation of size effect in concrete under uniaxial tension. In: Mihashi, H., Rokugo, K. (Eds.), FRAMCOS-3. Aedificatio Publishers, Japan, pp. 1923–1936.

van Vliet, M., van Mier, J., 1999. Effect of strain gradients on the size effect of concrete in uniaxial tension. International Journal of Fracture 95, 195–219.

van Vliet, M., van Mier, J., 2000a. Experimental investigation of size effect in concrete and sandstone under uniaxial tension. Engineering Fracture Mechanics 65, 165–188.

van Vliet, M., van Mier, J., 2000b. Size effect of concrete and sandstone. Engineering Fracture Mechanics 45, 91–108.

Vashy, A., 1892. Sur les lois de similitude en physique. Annales télégraphiques 19, 25–28.

Vořechovský, M., 2004a. Statistical alternatives of combined size effect on nominal strength for structures failing at crack initiation. In: Stibor, M. (Ed.), Problémy lomové mechaniky IV (Problems of Fracture Mechanics IV). Brno University of Technology, Academy of Sciences – Institute of Physics of Materials of the ASCR, pp. 99–106.

Vořechovský, M., 2004b. Stochastic fracture mechanics and size effect. Ph.D. thesis, Brno University of Technology, Brno, Czech Republic.

Vořechovský, M., in review. Simulation of cross correlated random fields by series expansion methods. Structural Safety.

Vořechovský, M., Chudoba, R., 2006. Stochastic modeling of multi-filament yarns: II. Random properties over the length and size effect. International Journal of Solids and Structures 43 (3–4), 435–458.

Vořechovský, M., Novák, D., 2005. Simulation of random fields for stochastic finite element analyses. In: Augusti, G., Schuëller, G.I., Ciampoli, M. (Eds.), ICoSSaR '05 the 9th International Conference on Structural Safety and Reliability. Millpress, Rotterdam, Netherlands, Rome, Italy, pp. 2545–2552.

Vořechovský, M., Bažant, Z.P., Novák, D., 2005. Procedure of statistical size effect prediction for crack initiation problems. In: Carpinteri, A. (Ed.), ICF XI 11th International Conference on Fracture. Politecnico di Torino, Turin, Italy, pp. CD–ROM proc, abstract page 1166.

Vořechovský, M., Chudoba, R., Jeřábek, J., 2006. Adaptive probabilistic modeling of localization, failure and size effect of quasi-brittle materials. In: Soares, C., Martins, J., Rodrigues, H., Ambrósio, J., Pina, C., Soares, C., Pereira, E., Folgado, J. (Eds.), III European Conference on Computational Mechanics (ECCM-2006). National Laboratory of Civil Engineering, Springer, Lisbon, Portugal, p. 286 (abstract), full papers on CD-ROM.

Weibull, W., 1939. The phenomenon of rupture in solids. Royal Swedish Institute of Engineering Research (Ingenioersvetenskaps Akad. Handl.), Stockholm 153, pp. 1–55.